

# Local charge to global structure in the face of disorder.

Carlos G. Oliver

Master of Science

Department of Biology

McGill University

Montreal, Quebec

June 19, 2016

A thesis submitted to McGill University in partial fulfillment of the requirements of  
the degree of Master of Science

©Carlos G. Oliver, 2016

## **DEDICATION**

This document is dedicated to the graduate students of the McGill University.

## **ACKNOWLEDGEMENTS**

Acknowledgments, if included, must be written in complete sentences. Do not use direct address. For example, instead of Thanks, Mom and Dad!, you should say I thank my parents.

## **ABSTRACT**

Abstract in English and French are required. The text of the abstract in English begins here.

## **ABRÉGÉ**

The text of the abstract in French begins here.

## TABLE OF CONTENTS

DEDICATION . . . . .	ii
ACKNOWLEDGEMENTS . . . . .	iii
ABSTRACT . . . . .	iv
ABRÉGÉ . . . . .	v
LIST OF TABLES . . . . .	viii
LIST OF ABBREVIATIONS . . . . .	ix
1 Introduction . . . . .	1
1.1 Disorder in proteins . . . . .	2
1.2 $\gamma$ -Tubulin . . . . .	3
2 Theory . . . . .	4
2.1 Molecular Dynamics Simulations . . . . .	4
2.1.1 Fixed-temperature Molecular Dynamics . . . . .	4
2.1.2 Replica Exchange Molecular Dynamics . . . . .	4
2.2 Evolutionary Algorithms . . . . .	4
3 Conformational analysis of the $\gamma$ -Tubulin carboxyl terminus . . . . .	5
3.1 NMR . . . . .	5
3.2 Setting up the MD runs . . . . .	5
3.3 Conformational sampling of $\gamma$ -CT isoforms . . . . .	6
4 MEDIEVAL . . . . .	15
5 Conclusions . . . . .	16
Appendix A . . . . .	17

Appendix B . . . . .	18
References . . . . .	19

LIST OF TABLES

<u>Table</u>	<u>page</u>
--------------	-------------

## LIST OF ABBREVIATIONS

<u>Figure</u>	<u>page</u>
3–1 Diffusion Coefficient . . . . .	8
3–2 Contact Maps . . . . .	10

## **CHAPTER 1**

### **Introduction**

Everything existing in the universe  
is the fruit of chance and necessity.

---

Democritus

Biological systems have evolved over billions of years to ensure their proper functioning in the face of ever changing environments. As a result, evolution has produced an immense diversity of highly robust systems/organisms of ever increasing complexity. Looking closely at these systems we find that at their heart is a complex network of molecular machines. Molecular machines are assemblies of protein macromolecules that interact in a highly coordinated manner to accomplish the various fundamental tasks to ensure survival of the organism in the eternal battle against entropy. These tasks encompass all the essential processes necessary for proper cellular functioning such as cell division, growth, nutrient transport, energy generation, immune response, etc. At the core of each of those processes is a highly complex and precise machine composed of countless interacting and inter-dependent proteins that work in concert to achieve a singular goal in a robust and flexible manner. For example, [Insert example of a complex molecular machine to show how complex and robust things are.] The primary aim of this thesis is to improve our understanding of the physical mechanisms underlying the functional complexity of molecular machines.

Looking closer at molecular machines, we see that their primary working unit is the protein. All communication between parts and functional output of the molecular machine occurs at the protein level. This activity is driven by the structural and dynamic properties encoded in each protein's amino acid sequence. Specific spatial arrangements of peptide chains and protein architectures allows for specific interactions between proteins to assemble molecular machines and recruit necessary factors. Consequently for a long time, the primary focus for trying to understand protein function was in describing the stable 3D architecture, or ordered folds that proteins adopt. In these efforts, techniques such as X-ray crystallography and electron microscopy have been very successful in describing the folded states of proteins and have led to many advances in understanding protein function. For example, [classical example of structure–function]. However, these techniques offer only a static picture of stable domains in proteins. We know that these protein systems. [example of dynamic protein system]. A static description of proteins is not sufficient to explain the degree of functional flexibility and control that we observe. How can a protein fulfill multiple functions without adopting multiple structural states? How can such molecular machines offer such precise control of functionality while counting only on a static architectures?

## 1.1 Disorder in proteins

Part of the answer can be found in regions of organized proteins that do not follow the classical structure-function dogma. These regions are known as intrinsically

disordered proteins or protein regions (IDPs/IDRs).<sup>1</sup> IDRs are segments of protein that do not natively adopt any stable conformation or fold. Instead, IDRs. are highly dynamic and rapidly sample different conformations. For a long time, these parts of proteins were overlooked in favour of studying stable folding patterns. IDRs were thought to act simply as flexible linkers between functional structural domains without any further function. This was also in part due to the fact that the main tool being used for structural biology, X-ray crystallography, fails to detect patterns in dynamic chains. While techniques that do produce information on dynamics such as NMR only developed for proteins until much later. The first protein structure solved by NMR was in 1984 by Kurt Wurtrich while the first protein structure solved by X-ray crystallography was in 1958 by J.C. Kendrew.

## 1.2 $\gamma$ -Tubulin

[Introduce gamma tubulin as a problem/puzzle where we need to understand how small changes in dynamics and conformational sampling can have broad impacts on an entire molecular machine.]

---

<sup>1</sup> There are several levels of disorder in proteins ranging from fully disordered proteins (IDPs), to local regions of disorder found within structured domains (IDRs). In this work we will focus on the latter.

## CHAPTER 2

### Theory

#### 2.1 Molecular Dynamics Simulations

##### 2.1.1 Fixed-temperature Molecular Dynamics

##### 2.1.2 Replica Exchange Molecular Dynamics

#### 2.2 Evolutionary Algorithms

## CHAPTER 3

### Conformational analysis of the $\gamma$ -Tubulin carboxyl terminus

In this chapter we discuss the impact of local charge on the global dynamics of the  $\gamma$ -Tubulin C-terminus ( $\gamma$ -CT). In order to measure how the addition of local negative charge in an acidic polypeptide affects the conformational sampling of the  $\gamma$ -CT, we simulated the dynamics of various isoforms of the  $\gamma$ -CT using MD. By comparing results from our simulations to experimental measurements performed with NMR spectroscopy on the  $\gamma$ -CT, we were able to propose that local changes in charge at specific residues in the polypeptide have the ability to bias the conformational sampling of the  $\gamma$ -CT in such a way that may be regulating the availability of binding surfaces on  $\gamma$ -Tubulin.

#### 3.1 NMR

Talk about NMR stuff here. ‘

#### 3.2 Setting up the MD runs

Molecular Dynamics simulations (MDS) on WT and Y11D  $\gamma$ -CTs were carried out using MPI-enabled GROMACS 4.6.6 software[2] and a CentOS 5 high performance computational cluster. Calculations were distributed over 64 Dual Sandy Bridge 8-core, 2.6 GHz computing nodes and run under periodic boundary conditions with the OPLS-AA (Optimized Potential for Liquid Simulations ? All Atom) force field [4]. The starting  $\gamma$ -CT polypeptide configurations were obtained from secondary and tertiary structure predictions by RaptorX [3] and solvated using the

SPCE (extended single point charge) water model in a dodecahedral box while enforcing a minimum distance between the edge of the box and solute of 1 nanometer. The total charge of the system was neutralized by adding sodium ions to the solution. Energy minimization was carried out using a steepest descent algorithm for a maximum of 50,000 steps until a maximum force of 100 kJ/mol between atoms was achieved. A 1 nm cut-off was used for non-bonded interactions, and long-range electrostatics were calculated using a Particle Mesh Edwald Sum algorithm. The systems equilibrated under the constant NVT and NPT ensembles (288K and 1 atm) for 5 ns before the production 2  $\mu$ s simulations. Post-processing of all trajectories was done using the `trjconv` module of GROMACS. Theoretical random-coil structural ensembles (10,000 conformers) were calculated based on the  $\gamma$ -CT primary amino acid sequence using Flexible Meccano software [5]. Translational diffusion coefficients were calculated for each structure using hydroNMR software [1]. MD conformations were grouped into percentile classes based on radius of gyration ( $R_g$ ) computed using the GROMACS `g_gyrate` module. Each  $R_g$  percentile group was represented by the three structures with lowest root-mean-squared-difference RMSD values to all other structures, calculated using the GROMACS `g_rms` module. Atomic distance matrices were calculated using the GROMACS `g_mdmat` module.

### 3.3 Conformational sampling of $\gamma$ -CT isoforms

Our NMR experiments provide evidence for a major alteration in the global dynamics of the  $\gamma$ -CT in the presence of the Y11D mutation characterized by collective motions involving the entire polypeptide chain occurring on the microsecond timescale. We then asked whether this phenomenon can be reproduced *in silico* using

MDS. If we are able to reproduce the transition *in silico*, the resulting MD data can be used to obtain additional insight into the structural characteristics of the conformational sampling of the  $\gamma$ -CT at an atomic resolution. We computed trajectories for the WT and Y11D  $\gamma$ -CT polypeptides by running independent  $2\mu\text{s}$  GROMACS simulations, and computed the translational diffusion coefficient from the resulting MDS structural trajectories at 1 ns time steps **Fig. 3.3**. We found that the diffusion coefficient ( $D_c$ ) of the WT  $\gamma$ -CT remains relatively constant over the total simulation time ( $D_c = 1.237 \times 10^{-6} \pm 1.5816 \times 10^{-8} \text{ cm}^2 \text{ s}^{-1}$  and agrees well with the NMR-derived value ( $D_c = 1.25 \times 10^{-6} \pm 1 \times 10^{-8} \text{ cm}^2 \text{ s}^{-1}$ ). Similarly to what was seen by NMR, we find that the mean  $D_c$  of the Y11D  $\gamma$ -CT polypeptide is slightly lower than that of the WT  $\gamma$ -CT ( $D_c = 1.224 \times 10^{-6} \pm 3.503 \times 10^{-8} \text{ cm}^2 \text{ s}^{-1}$ ). These results confirm that the  $\gamma$ -CT, while disordered, is more compact than a fully denatured polypeptide chain. Interestingly, between 762 to 1255 ns in the MDS, the Y11D  $\gamma$ -CT underwent transient excursions to less compact conformations with significantly lower diffusion coefficients (mean  $D_c = 1.152 \times 10^{-6} \pm 2.0325 \times 10^{-8} \text{ cm}^2 \text{ s}^{-1}$ ). This sub-population is more extended (i.e. diffuses more slowly) than any conformation sampled by the WT  $\gamma$ -CT throughout the entire MDS. While the Y11D  $\gamma$ -CT extended states do not overlap with the conformational ensemble of the WT  $\gamma$ -CT polypeptides, they do, however, lie within the conformational space expected for a typical random-coil polypeptide, as modeled by an ensemble of 10,000 disordered extended conformers (Fig. S8) derived from the  $\gamma$ -CT primary sequence using the **Flexible Meccano** tool.

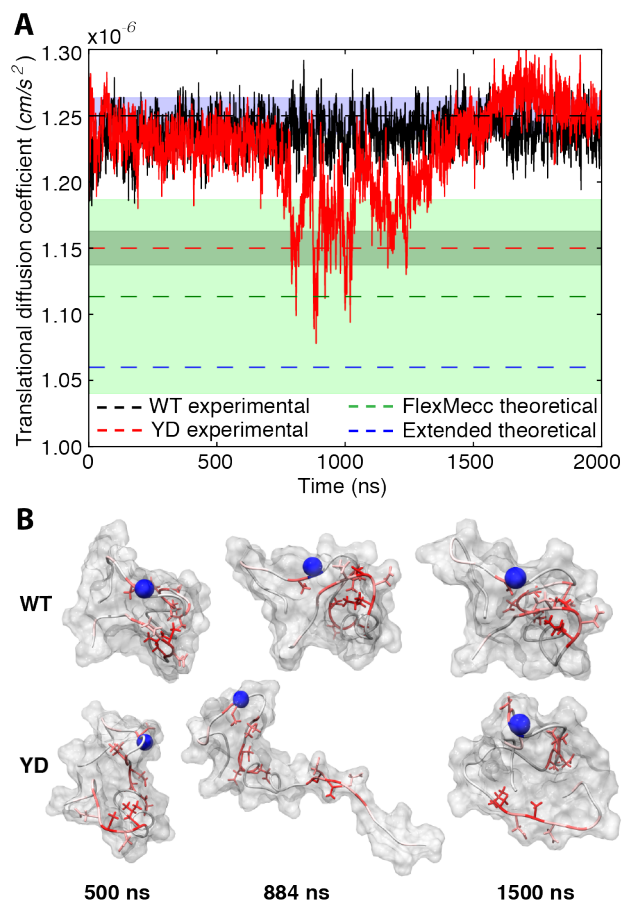


Figure 3–1: Diffusion Coefficient

In order to obtain an initial visualization of the transient opening motions experienced by the Y11D polypeptide, we extracted structural models from the simulation at the time step with the lowest value of D<sub>s</sub> for the Y11D  $\gamma$ -CT polypeptide (844 ns;  $D_c = 1.078 \times 10^{-6} \text{ cm}^2 \text{ s}^{-1}$ ) as well as the time steps at 500 ns ( $D_c = 1.268 \times 10^{-6} \text{ cm}^2 \text{ s}^{-1}$  for WT and  $1.235 \times 10^{-6} \text{ cm}^2 \text{ s}^{-1}$  for Y11D) and 1500 ns ( $D_c = 1.233 \times 10^{-6} \text{ cm}^2 \text{ s}^{-1}$  for WT and  $1.241 \times 10^{-6} \text{ cm}^2 \text{ s}^{-1}$  for Y11D). The expansion experienced by the Y11D polypeptide is clearly observed in the 844 ns structure. We hypothesize that the global microsecond dynamics characterized by NMR for the Y11D  $\gamma$ -CT correspond to the transient opening motions seen by MDS, with the major state corresponding to the compact form and the minor state corresponding to the expanded form. Residues with large-magnitude dispersion profiles (i.e. those in Figure 6 with large  $\Delta R_2$ ) have chemical shifts that are quite different in the major and the minor states. If the NMR dynamics correspond to transient expansion, these residues should experience different local environments in the collapsed and expanded states. Residues with large  $\Delta R_2$  values (coloured red in Figure 7B) indeed are located in a compact cluster at 500 ns for the Y11D  $\gamma$ -CT and at all time steps for the WT  $\gamma$ -CT. However during expansion, this cluster dissociates and the residues become more solvent-exposed. This provides a possible explanation for how residues throughout a disordered polypeptide can experience a concerted, two-state, dynamical process presence of the Y11D mutation, and suggests that it is the separation of a cluster of residues located in N and C termini of the  $\gamma$ -CT polypeptide that drives a transition to extended conformations with a concomitant reduction of the translational diffusion coefficient.

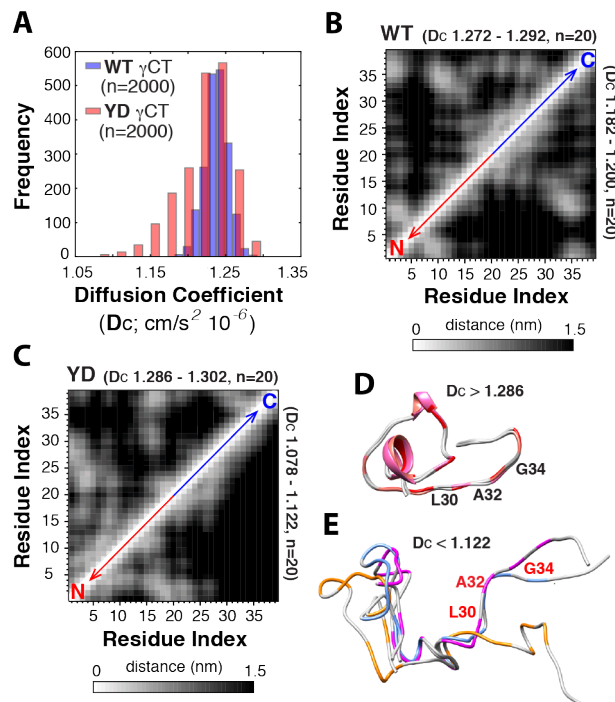
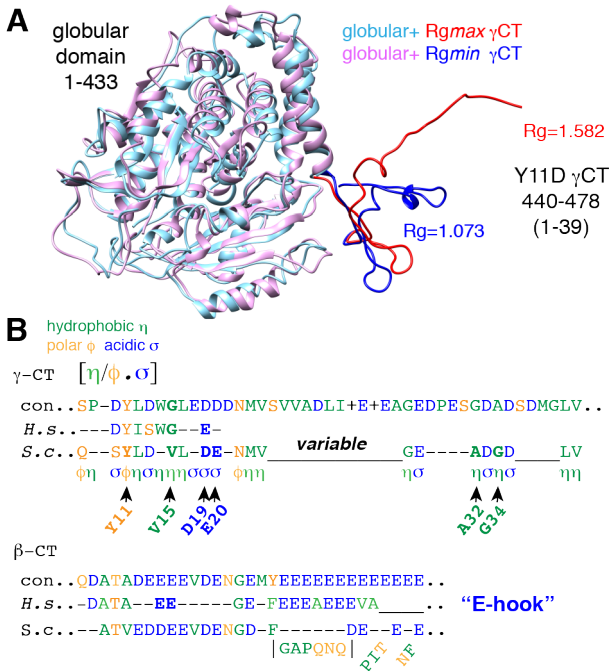


Figure 3–2: Contact Maps

To further characterize the transition observed in the Y11D  $\gamma$ -CT polypeptide, we chose a subset of 2000 time steps (every 1 ns) for additional analysis. We calculated theoretical diffusion coefficients for each structure, yielding the frequency histograms shown Figure 8A. The Y11D  $\gamma$ -CT distribution is clearly skewed compared to that of the WT with many structures exhibiting far slower self-diffusion and more extended conformations. The conformations within the top and bottom 1% (20 structures each) of the WT  $\gamma$ -CT and Y11D  $\gamma$ -CT Ds distributions best represent the collapsed (top 1%) and extended (bottom 1%) conformations for  $\gamma$ -CT polypeptides. In the case of the WT, we do not expect the upper and lower Ds subsets to substantially differ, as the WT  $\gamma$ -CT conformations exhibit fairly homogenous compactness overall. For Y11D  $\gamma$ -CT, we expect the upper Ds subset to resemble that of the WT  $\gamma$ -CT, while the lower Ds subset is expected to reflect the transient opening process. We plotted the mean distance between alpha carbons of all pairs of residues for as contact maps for the set of collapsed (upper) and extended (lower) conformations of the WT  $\gamma$ -CT polypeptide (Fig. 8B) and the Y11D  $\gamma$ -CT polypeptide (Fig. 8C). As expected, the upper and lower Ds subsets of the WT  $\gamma$ -CT and the upper Ds subset of the Y11D  $\gamma$ -CT polypeptides show similar patterns of pair-wise contacts. In contrast, the C-terminal residues in the lower Ds subset of the Y11D  $\gamma$ -CT lose the majority of contacts with N terminal residues, as a consequence of the conformational expansion. Next, we isolated the three conformations from the upper and lower Ds subsets of Y11D  $\gamma$ -CT polypeptides with the lowest all-to-all RMS, also known as centroid structures, shown in Fig. 8D,E. with large relaxation

dispersion magnitudes indicated in red. This analysis shows that the extended conformations consist of a compact N-terminus with residues located in the C-terminal region of the  $\gamma$ -CT, (including dynamically-broadened residues L30, A32 and G34) isolated from the N-terminus and solvent-accessible. Through MDS we are able to re-produce the anomalously rapid diffusion (i.e. high compactness) of the WT and Y11D ground-state  $\gamma$ -CT polypeptides. Moreover, we saw that the Y $\downarrow$ D substitution caused relatively slow collective motions of the entire polypeptide chain, as observed by NMR.

Representative structures obtained identifying structures with lowest all-to-all RMSD values for the YD high diffusion coefficient group (D) and YD low diffusion coefficient group (E), residues with  $\Delta R_2$  values greater than 5 s<sup>-1</sup> are labeled in red. Our experimental analysis of the structural properties of the  $\gamma$ -CT using NMR and corresponding MDS are based on the properties of the WT and Y11D  $\gamma$ -CT polypeptides in isolation. In order to determine whether the conformations and dynamics we observed for the isolated ??CTs are physically consistent within the context of the full-length  $\gamma$ -tubulin protein, we docked the minimum Ds  $\gamma$ -CT model (Fig. S9) onto the globular domain of an S.c.  $\beta$ -tubulin homology model and used this as an initial structure for whole protein simulations on  $\gamma$ ?tubulin. Due to the increase in system size, simulation times were reduced to 200ns. As with the Y11D  $\gamma$ -CT polypeptide, the  $\gamma$ -CT in the whole protein simulation underwent exchange between extended and compact conformations (Fig. S10), suggesting both states are accessible in the presence of the globular domain. We found no contacts between residues in the globular domain with the 39 residues of the  $\gamma$ -CT throughout the 200



ns simulation (minimal distance between any pair of residues is  $\geq 0.7$  nm). Structures for the full protein with the  $\gamma$ -CT at minimum radius of gyration (1.073 nm; model S11) and maximum radius of gyration (1.582 nm; model S12) are shown in Fig. 9A.

The CTs of  $\alpha$ -  $\beta$ - and  $\gamma$ -tubulins are enriched in acidic residues (Asp, Glu).  $\gamma$ -CTs across eukaryotes additionally contain clusters of hydrophobic or polar residues which are not found in  $\alpha$ - or  $\beta$ -CTs. Interestingly, the residues most broadened in Y11D NMR spectra, i.e. those most affected by the compact-to-extended transition (V15, D19, E20, A32, G34), are all found in positions conserved either on a sequence level or on a physical property level (polarity/charge) in a consensus  $\gamma$ -CT sequence (Fig. 9B). This suggests that clusters of hydrophobic residues, including those that contribute to transitions between compact and extended conformations

in the S.c. D11  $\gamma$ -CT, are a feature of an otherwise diverse set of  $\gamma$ -CT s across many eukaryotic organisms.

## **CHAPTER 4**

### **MEDIEVAL**

?A totally blind process can by definition lead to anything; it can even lead to vision itself.? Jacques Monod

## **CHAPTER 5**

### **Conclusions**

## **Appendix A**

Here is the text of an Appendix.

## **Appendix B**

Here is the text of a second, additional Appendix

## References

- [1] J Garcia De la Torre, ML Huertas, and B Carrasco. Hydronmr: prediction of nmr relaxation of globular proteins from atomic-level structures and hydrodynamic calculations. *Journal of Magnetic Resonance*, 147(1):138–146, 2000.
- [2] Berk Hess, Carsten Kutzner, David Van Der Spoel, and Erik Lindahl. Gromacs 4: algorithms for highly efficient, load-balanced, and scalable molecular simulation. *Journal of chemical theory and computation*, 4(3):435–447, 2008.
- [3] Morten Källberg, Haipeng Wang, Sheng Wang, Jian Peng, Zhiyong Wang, Hui Lu, and Jinbo Xu. Template-based protein structure modeling using the raptortx web server. *Nature protocols*, 7(8):1511–1522, 2012.
- [4] George A Kaminski, Richard A Friesner, Julian Tirado-Rives, and William L Jorgensen. Evaluation and reparametrization of the opls-aa force field for proteins via comparison with accurate quantum chemical calculations on peptides. *The Journal of Physical Chemistry B*, 105(28):6474–6487, 2001.
- [5] Valéry Ozanne, Frédéric Bauer, Loïc Salmon, Jie-rong Huang, Ma-lene Ringkjøbing Jensen, Stéphane Segard, Pau Bernadó, Céline Charavay, and Martin Blackledge. Flexible-meccano: a tool for the generation of explicit ensemble descriptions of intrinsically disordered proteins and their associated experimental observables. *Bioinformatics*, 28(11):1463–1470, 2012.